GEOFIZIKA VOL. 39 2022

DOI: https://doi.org/10.15233/gfz.2022.39.9
Original scientific paper

Prediction of bimodal monsoonal rainfall in the central dry zone of Myanmar using teleconnections with global sea surface temperatures

Hiroshi Yasuda [1], *Ayele Almaw Fenta* [2], *Hidetoshi Miyazaki* [3], *Shun Ishiyama* [4], *Koji Inosako* [5], *Aung Din* [6] *and Takayuki Kawai* [7]

[1] Organization for Educational Support and International Affairs, Tottori University, Tottori, Japan

[2] Arid Land Research Center, Tottori University. Tottori, Japan

[3] Global Environmental Forum, Tokyo, Japan

[4] National Museum of Ethnology, Osaka, Japan

[5] Faculty of Agriculture, Tottori University, Tottori, Japan

[6] Nature Lovers International, Yangon, Myanmar

[7] Graduate school of International Resource Sciences, Akita University, Akita, Japan

Received 16 July 2021, in final form 24 March 2022

In the central dry zone of Myanmar, the mean annual rainfall is less than 1000 mm. Although rainfed agriculture is commonly practiced there, the feasibility of rainfed farming is compromised by the large fluctuations of rainfall and the frequent occurrence of dry years. The monthly distribution of rainfall follows a bimodal pattern. The intensity of the monsoonal rainfall from May to October is characterized by two peaks, an early peak (May–June) and a late peak (August–October), separated by the inter-monsoon (July). The return times of dry and wet years make management of rainfed agriculture problematic. There is very little correlation between the early and late monsoonal rainfall ($r = -0.257$). However, monsoonal rainfall is teleconnected to sea surface temperatures (SSTs) in certain areas of the Pacific Ocean in real time. Furthermore, at lag times of 6–9 months, there are teleconnections between the early monsoonal, inter-monsoonal, and late monsoonal rainfall and SSTs in certain areas of the Indian Ocean and Atlantic Ocean. We used an Elman artificial neural network model to predict early monsoonal, inter-monsoonal, and late monsoonal rainfall based on teleconnections with SSTs in the Indian and Atlantic oceans 6–9 months before the rainfall occurred. The correlation coefficient between the predicted and observed rainfall exceeded 0.7 in all three cases.

Keywords: artificial neural network, bimodal rainfall, inter-monsoon, Myanmar central dry zone, rainfed agriculture

1. Introduction

Myanmar, which is located in Southeast Asia, is well known for its rice cultivation and monsoonal climate (Herridge et al., 2019). The southwestern monsoon from the Bay of Bengal is the main source of rainfall during the rainy season. The annual rainfall, which averages a few thousand millimeters in the southern coastal area and northern mountains, is associated mainly with the southwestern monsoon (Roy and Kaur, 2000). In contrast, the annual rainfall is less than 1000 mm in the central part of Myanmar because the monsoon is intercepted by the Arakan Mountains in western Myanmar, and central Myanmar lies in the rain shadow of those mountains. Rain-fed agriculture is the mainstay of Myanmar's economy (Poe, 2011), but the country's agricultural practices are strongly affected by the amount and timing of monsoonal rainfall (Roy and Roy, 2011).

Roy and Kaur (2000) have identified homogenous rainfall zones across Myanmar based on the annual rainfall in monsoon months (June to September). Among these zones, the central dry zone (CDZ) receives the least rainfall. The CDZ comprises large areas of agricultural lands where mainly drought-tolerant crops are cultivated. Although the middle reach of the Ayeyarwady River, the main river in Myanmar, flows through the CDZ, farming in central Myanmar is based mainly on rainfall because of a lack of irrigation facilities. Farming in central Myanmar is therefore constrained by the limited amount of rainfall (Poe, 2011). In the CDZ, the amount of rainfall and the timing of the rainy season fluctuate greatly from year to year (Japan International Cooperation Agency, 2010). The low average rainfall therefore constrains agricultural production, and the interannual variability of rainfall confounds stabilization of that production. Moreover, because the traditional agricultural technology in Myanmar has been developed mostly for paddy fields and a monsoonal climate, the technology for field farming under dry conditions is relatively immature. In sum, agricultural productivity in the CDZ is greatly constrained by the amount and variability of rainfall, and farmers there face the risk of dry years. An ability to predict the characteristics of rainfall is therefore required for effective management of farms in central Myanmar and would be expected to greatly benefit rainfed agriculture in the CDZ.

Studies of the application of teleconnections based on global sea surface temperatures have been carried out with the goal of predicting rainfall (*e.g.*, Uvo et al., 1998; Ahmed et al., 2008; Mondal et al., 2011; Kumbuyo et al., 2014; Shahi et al., 2018; Yasuda et al., 2018; Shahi et al., 2016; Shahi et al., 2019; Shahi et al., 2020). Sea surface temperature (SST) teleconnections are reliable indicators of meteorological variables such as temperature, humidity, and precipitation. The Spanish terms, El Niño and La Niña, often appear in long-term weather forecasts. Each indicates an SST phase in the equatorial Eastern Pacific Ocean (off Peru). El Niño and La Niña are phases of the El Niño–Southern Oscillation (ENSO) cycle, and the patterns of that cycle have been used to predict weather anomalies. Yasunari (1990) has reported a link between the Asian sum-

mer monsoon and conditions in the tropical Pacific Ocean and the tropical Pacific atmosphere.

Because Myanmar faces the Indian Ocean, a relationship between SSTs throughout the Indian Ocean and rainfall in Myanmar is expected. The Indian Ocean Dipole (IOD) is the difference between SST in the western and eastern Indian Ocean. Sein et al. (2015) have shown that there is a negative correlation between the IOD and monsoonal rainfall over Myanmar. Shahi et al. (2019) have identified SST predictors based on spatial patterns of correlation coefficients between summer monsoonal rainfall in India and SST over the Indian and Pacific oceans.

The general definition of a monsoon is a wind system that undergoes a seasonal 180° reversal of direction for any reason whatsoever. Onshore summer winds are moisture-laden and produce heavy coastal rainfall, especially along the Indian Ocean (Eagleson, 1970). Monsoonal rainfall in coastal areas of Myanmar is generated by the moisture-laden wind from the Indian Ocean.

Toe et al. (2017) have adopted the term "climatological monsoon break," introduced by Takahashi and Yasunari (2006), to describe the seasonal pattern of rainfall in the CDZ of Myanmar. The climatological monsoon break is a transitional period during which rainfall dynamics change from a monsoon to a tropical depression over Indochina, and it begins in late June. The climatological monsoon break is synchronized with a change of large-scale monsoonal circulation over Indochina and divides the rainy season into an early and late monsoon. Because the processes responsible for rainfall dynamics during the early and late monsoons differ, there is no relationship between the two monsoon seasons.

This goal of this study was to reveal the characteristics of rainfall over the CDZ of Myanmar and the teleconnections between that monsoonal rainfall and SST. The data and methodology used in the present work are described in section 3, Data and methodology. Details of the rainy season are described in sections 4.1.–4.3., and sections 4.4. and 4.5. describe the teleconnections between monsoonal rainfall and SSTs. Section 4.6. describes use of an artificial neural network to predict monsoonal rainfall from teleconnections.

2. Study area

The CDZ is a relatively low-lying area in the middle of Myanmar that covers an area of about 60×10^3 km^2 (Fig. 1) within latitudes 19.5–23.3° N and longitudes 94.3–96.4° E. The region is home to an estimated 12 million people and provides 35% of Myanmar's grain cropping, but it is still underdeveloped (Herridge et al., 2019). The CDZ is a center of rainfed, upland cropping systems, which are vulnerable to variations of rainfall. It is thus one of the most food-insecure, water-stressed, climate-sensitive, natural resource–poor, and least-developed regions of Myanmar (Asian Development Bank, 2016). The CDZ is a climatic

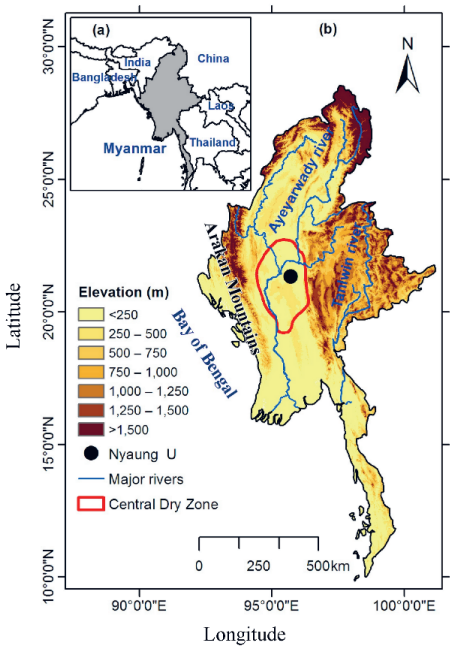

Figure 1. The central dry zone in Myanmar.

geographical location defined as an area where annual rainfall is less than 1000 mm. The area is shielded by high mountains along its western and eastern boundaries; the Ayeyarwady River and major tributaries flow from north to south through the CDZ (Fig. 1).

3. Data and methodology

3.1. Rainfall and SST data

Monthly rainfall data (1980–2015) for the city of Nyaung-U in the CDZ were obtained from the National Meteorological Authority, Myanmar (Fig. 1).

Monthly global SST data were obtained from the Hadley Centre Global Sea Ice and Sea Surface Temperature (HadISST) dataset (Rayner et al., 2003, 2006). The HadISST dataset, which is provided by the Meteorological Office of the United Kingdom, contains monthly, globally complete fields of SST on a 1° latitude–longitude grid from 1870 to the present and has been used in numerous previous studies (*e.g.*, Chhin et al., 2019; Alhamshry et al., 2019, 2020). Because the rainfall data spanned the years 1980–2015, we used SST data from 1979 to 2015 to predict rainfall up to 10 months later.

We used standardized data for the analysis in this study. To evaluate seasonal rainfall and the correlation between rainfall and SST, we used the interannual time series of standardized rainfall and SST.

3.2. Return period

Whether rainfall is more or less than mean rainfall is a crucial factor in rainfed agriculture. Estimation of the return periods of wet and dry years is essential for planning agricultural activities in the CDZ. In this study, wet and dry years were defined as years when rainfall was more and less than the mean, respectively.

The exceedance and non-exceedance probabilities of monsoonal rainfall were evaluated to predict wet and dry years, respectively. For the early (May–June) and late (August–October) monsoon seasons, return periods of dry years were evaluated.

Inter-monsoon (July) rainfall is critical for rainfed farming because it determines whether crop cultivation is interrupted. Return periods of wet years were evaluated for inter-monsoon seasons. To estimate return periods, we assumed that the interannual time series of early monsoonal, inter-monsoonal, and late monsoonal rainfall followed lognormal distributions (Bonaccorso et al., 2003; Rugumayo and Mwebaze 2007; Yusof et al., 2013).

A lognormal distribution was used to estimate the exceedance probability per year (p) that rainfall would exceed a given rainfall, and the return period T was defined as the inverse of the exceedance probability, *i.e.*, $1/p$. The non-exceedance probability was equated to $1 - p$. The exceedance and non-exceedance probabilities were applied to estimate the return periods for wet and dry years, respectively.

3.3. Correlation analysis

We calculated correlation coefficients between rainfall and global SST to identify teleconnections between SST and monsoonal rainfall. We calculated Pearson product-moment correlation coefficients (r values) between monsoonal rainfall and SST for lag times ranging from 0 to 10 months (*e.g.*, Smith et al., 2000; Kumbuyo et al., 2014). A Student's t test against the null hypothesis of no correlation was used to assess statistical significance (Lloyd-Hughes and Saunders, 2002). For the correlation calculation, we standardized the interannual time series of rainfall and global SST data with the mean and standard deviation as follows:

$$X_i = \frac{(x_i - \mu)}{\sigma}, \tag{1}$$

where X_i, x_i, μ, and σ are the standardized value, raw value, mean, and standard deviation, respectively.

The lag times of the correlation analysis were chosen based on average conditions during the duration of the early and late monsoons. We calculated the correlations with values averaged over the durations of the early monsoon (May to June) and late monsoon (August to October) with averaged values of time-lagged SSTs.

Correlations were evaluated for lag times of 0 month (real time) and several months (Alhamshry et al., 2019). Strong correlations in real time indicate a synchronized teleconnection between monsoonal rainfall and SST. Strong correlations at lag times of several months can be used to predict rainfall.

3.4. Artificial Neural Network (ANN)

An artificial neural network (ANN) model was constructed to predict monsoonal rainfall using the teleconnections between monsoonal rainfall and SST. Artificial neural networks have been used to reconstruct meteorological and hydrological phenomena (*e.g.*, Sfersos and Coonick, 2000; Uvo et al., 1998, 2000; Olsson et al., 2001; Goyal and Ojha, 2012). An ANN model is an optimized system that connects the input and output through simple, interconnected processing neurons arranged in layers. After a long series of trial-and-error tests, Uvo et al. (2000) found that a three-layer, feed-forward ANN made the most accurate predictions of river discharges in Amazonia. Various structures of ANN models have been developed, and the three-layer structure is most commonly used in the fields of meteorology and hydrology. An ANN can connect two different variables related in a highly nonlinear manner because the ANN does not require information on system dynamics. ANNs have therefore been used in a variety of fields because of their versatility in identifying relationships between two variables (*e.g.*, Bishop, 1995; Uvo et al., 2000; Dash et al., 2010: Yuan et al., 2016; Yasuda et al., 2018: Alhamshry et al., 2019).

In this study, we used an Elman neural network model, a three-layer model in which the input layer represented SSTs, and the analysis in the middle (hid-

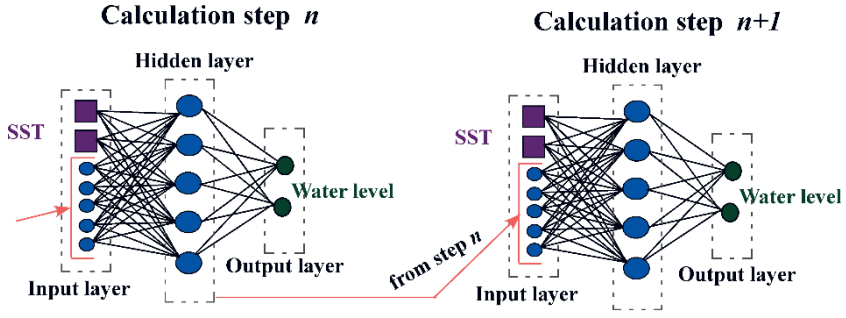

Figure 2. The structure of the Elman artificial neural network model. The output of the hidden layer at one step is transferred to the input layer of the next step.

den) layer was carried forward to calculate the amount of rainfall, as shown in Fig. 2. The Elman neural network is a recurrent system (Elman, 1990). The output of the hidden layer at one time step is fed back to the input layer at the next time step. An Elman ANN is a powerful tool for modeling time series wherein the output of the hidden layer at step (n) is transferred to the input of the network for the next step ($n+1$). We used data from 1980 to 1997 to train the network (the training span). The calculated rainfall in the output layer was compared with the observed rainfall, and the weight factors were renovated by using a back-propagation algorithm (*e.g.*, Bishop, 1995). The optimized weight factors were then applied to the data from 1998 to 2015 (the application span). The final optimization was based on the best fit (strongest correlation) to the rainfall data for the period 1980–2015.

4. Results and discussion

4.1. Monsoon season

Figure 3a shows the time series of annual rainfall from 1980 to 2015. The mean was 633 mm, and the coefficient of variation (*CV*) was 0.253. The *CV* is defined as the ratio of the standard deviation to the mean (*e.g.*, Kumbyo et al., 2014; Yasuda et al., 2018; Alhamshry et al., 2019). As the *CV* indicates, the interannual variation was large. The minimum annual rainfall during the study

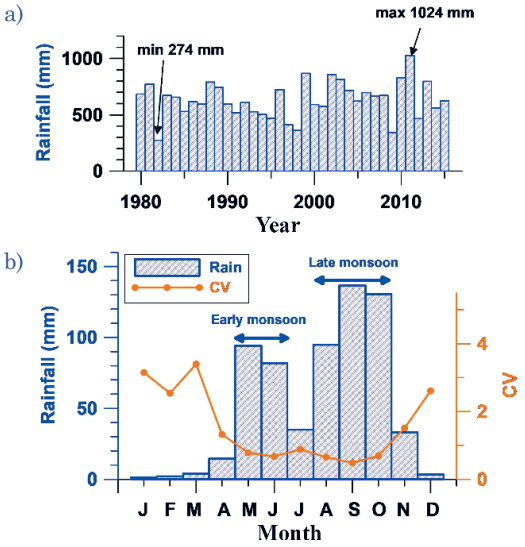

Figure 3. Time series of annual rainfall (*a*) and monthly mean rainfall and coefficient of variation (*CV*) of monthly mean rainfall (*b*).

period was 274 mm in 1982, and the maximum was 1024 mm in 2011. The maximum was thus four times the minimum.

Figure 3b shows the monthly mean rainfall and *CV*. The bimodal pattern of rainfall reflects the fact that the rainy season is divided into two periods that are associated with the early and late monsoons. The mean rainfall during the early, inter-, and late monsoon was 176, 35, and 362 mm, respectively. These variable amounts of rainfall indicate why rainfed agriculture in the CDZ of Myanmar is problematic. The total rainfall of 573 mm from May through October suggests that there is adequate rainfall to support rainfed agriculture. However, the CDZ receives less rainfall overall than the rest of Myanmar, and the bimodal pattern of monthly rainfall further constrains rainfed agriculture in the CDZ. The inter-monsoonal rainfall is the critical factor that determines the success of rainfed agriculture because the whole monsoon season (farming period) is interrupted by the inter-monsoon. The success of rainfed agriculture is very sensitive to conditions during the inter-monsoon season, including its onset, duration, and the occurrence of dry spells. Prolonged dry spells during the inter-monsoon season have devastating effects on farming in the CDZ. The different meteorological dynamics during the early and late monsoon are separated by the climatological monsoon break in June (Takahashi and Yasunari, 2006; Toe, 2017). The onset of the transition of the coupled ocean-atmospheric dynamics in the Indian Ocean at the end of June brings the inter-monsoon.

The rainfall during the inter-monsoon (July) was quite low and underwent remarkable interannual variations (Fig. 4): the mean of the inter-monsoonal rainfall was only 35 mm, and the *CV* was 0.883. Rainfall during July was often less than 10 mm in the CDZ. Although the amount of rainfall required for rainfed agriculture depends on the kind of crop, soil properties, potential evapotranspiration, temperature, and other meteorological factors, rainfall of approximately 250–350 mm during the farming period is considered to be the standard (Graef and Haigis, 2001; FAO, 2011). Requirements of 10 mm/week (40 mm/month) and 20 mm/10 days (60 mm/month) have also been reported (Deka and Nath, 2000; Singh et al., 2008; Nyakudya and Stroosnijder, 2011). The mean rainfall during July of 35 mm is therefore less than the amount of rainfall required for rainfed

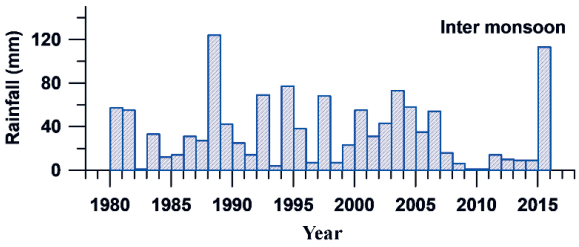

Figure 4. Interannual time series of inter-monsoonal (July) rainfall.

farming. Rainfall in July was less than 40 mm during 13 of the 36 years in the time series (Fig. 4). Rainfed farming is therefore often problematic during July in the CDZ.

4.2. Return periods of dry and wet years

The application of lognormal distributions to the monsoonal rainfall led to the return periods of dry years for the early and late monsoons shown in Tab. 1a. Rainfall during five dry years averaged 116.6 mm and 243.4 mm in the early and late monsoon, respectively (about two-thirds of the mean). These low amounts of rainfall resulted in no harvest.

Table 1b shows the return periods for wet inter-monsoon years. Because the whole monsoon season is interrupted by the inter-monsoon, rainfall during the inter-monsoon is the most sensitive determinant of agricultural productivity. The early monsoonal rainfall of 176.1 mm over a period of two months is not enough for rainfed agriculture. If rainfall during the following inter-monsoon is sufficient (*i.e.*, $\geq$ 40 mm), cultivation continues through the late monsoon. The amounts of rainfall in July corresponding to wet return periods of 3 and 4 years were 38.6 and 56.6 mm, respectively. Rainfall during the inter-monsoon was therefore adequate for rainfed agriculture once every 3–4 years. The estimated return period of 3–4 years indicates that rainfed agriculture is highly vulnerable to rainfall in the CDZ.

Table 1a. Return periods of dry periods (non-exceedance probability).

	Return period (years)	3	5	10	20	30
Early monsoon	Rainfall (mm)	131.8	116.6	102.3	91.8	86.8
Late monsoon		285.2	243.4	205.5	178.7	166.1

Table 1b. Return periods of wet periods (exceedance probability).

	Return period (years)	3	4	5	10	20	30
Inter-monsoon	Rainfall (mm)	38.6	56.6	71.2	112.6	141.6	152.8

4.3. Relationship between the early and late monsoons (wet and dry phases of the monsoonal rainfall)

To evaluate the rainfall during early monsoon (May–June), inter-monsoon, and late monsoon (August–October), we used Eq. (1) to standardize the inter-annual time series of total rainfall during each period. Figure 5 shows the standardized rainfall during the early and late monsoons to help elucidate the relationship between them. Amounts of rainfall above (positive) and below (negative) the mean indicate wet and dry phases, respectively. Using the standardized rainfall, we characterized each early and late monsoon season as wet or dry.

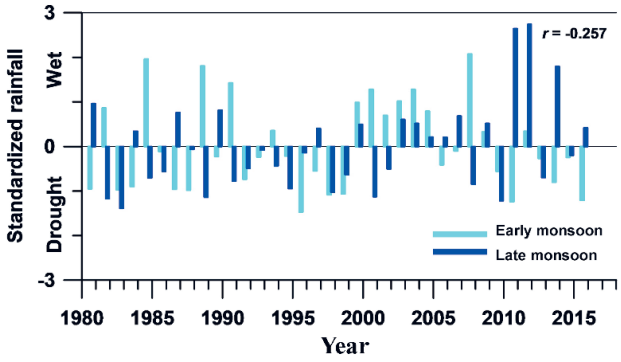

Figure 5. Time series of standardized rainfall during the early and late monsoons. Positive and negative values indicate wet and dry phases, respectively.

The patterns of the two monsoons were quite different. The correlation coefficient between the two was −0.257 and was not statistically significant. Wet conditions during one monsoon and dry conditions during the other in the same year occurred 18 times in 36 years. The amount of rainfall during the late monsoon could therefore not be estimated from the amount of rainfall during the early monsoon. The monsoon season was clearly divided by the inter-monsoon.

4.4. Teleconnection at a lag of 0 month (real time)

Absolute values of correlation coefficients $|r| \geq 0.43$ and $|r| \geq 0.52$ were statistically significant at $p = 0.01$ and 0.001, respectively. In this study, SST zones with $|r| \geq 0.43$ were identified as teleconnected zones. A strong correlation at a lag time of 0 month indicates a teleconnection in real time.

We calculated the correlation coefficients between monsoonal rainfall and SST at a lag of 0 month. The left side of Fig. 6 shows the oceanic areas where the SST was significantly correlated ($p < 0.01$) with monsoonal rainfall. In the case of the early monsoon, the correlations were significant over large areas of the Pacific Ocean. The correlations were positive over the central, subtropical North Pacific and negative over the eastern equatorial Pacific and Humboldt Current system. The significant negative correlations throughout the eastern equatorial Pacific and off the coast of Peru suggested La Niña conditions. Roy and Roy (2011) have previously reported a close association between rainfall over the CDZ of Myanmar and SSTs in the Pacific Ocean during the La Niña phase of the ENSO. Sein et al. (2015) have previously shown that La Niña induces wet conditions during the summer in Myanmar.

In addition to the Pacific Ocean, there were negative correlations between early monsoonal rainfall and SST in some areas of the Indian Ocean, particularly to the east of Madagascar. These correlations suggested a relationship to the IOD. Inter-monsoonal rainfall was positively correlated with SST in the

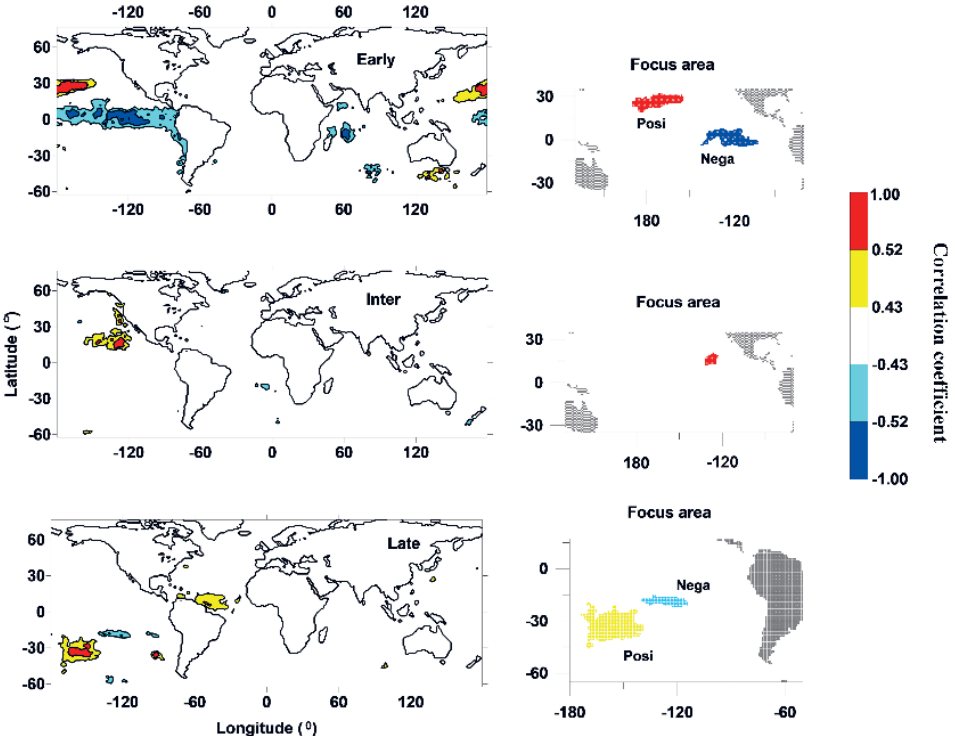

Figure 6. Areas where correlations between sea surface temperatures (SSTs) and monsoon rainfall were significant in real time. $|r| > 0.43$ and $|r| > 0.52$ indicate $p < 0.01$ and $p < 0.001$, respecttively (*left*). Focus areas where there were significant correlations between SST and rainfall (*right*).

eastern, low-latitude region of the Pacific Ocean off the coast of Mexico and west coast of the United States. Rainfall during the late monsoon was positively correlated with SST in the temperate, southeastern Pacific and equatorial Atlantic off the northeastern coast of South America; it was negatively correlated with SST in the subtropical, southeastern Pacific.

Whereas the early monsoonal rainfall was strongly and negatively correlated with the SST of the eastern equatorial Pacific, there was no similar correlation with the late monsoonal rainfall. The climatological break between the early and late monsoons over Indochina is a transitional period that changes rainfall dynamics from a monsoon to a tropical depression over Indochina, and it begins in late June (Takahashi and Yasunari, 2006; Toe et al., 2017). The climatological break is synchronized with a change of the large-scale monsoonal circulation over Indochina and divides the rainy season into the early and late monsoons. Because the processes responsible for rainfall dynamics during the early and late monsoons differ, there is no relationship between the two monsoon seasons, and the meteorological dynamics of the early and late monsoons differ.

The right side of Fig. 6 shows the central zones of the areas of correlated SSTs. Figure 7 shows time series of the spatial averages of the SSTs in these focus areas (*i.e.*, the right side of Fig. 6) and monsoonal rainfall. Figure 7 (a) shows time series of positively correlated SSTs, negatively correlated SSTs, and the difference (positively correlated minus negatively correlated SSTs) along with early monsoonal rainfall. Yasuda et al. (2018) have reported that the differences between the SSTs in zones where SSTs are positively and negatively correlated with rainfall (*i.e.*, an SST dipole) is more strongly correlated with rainfall than the SSTs themselves. The positive and negative correlation coefficients of the SST zones were 0.620 and −0.574, respectively; the correlation coefficient between the SST difference and rainfall was 0.643.

The spatial average of SST over the eastern equatorial Pacific off the west coast of Mexico was positively correlated with inter-monsoonal rainfall ($r = 0.597$, $p < 0.01$). In the temperate southeastern Pacific, there were separate areas where the SST was either positively or negatively correlated with late monsoonal rainfall (Fig. 7c). This pattern is similar to the pattern of the correlations between SSTs in the northeastern Pacific and early monsoonal coefficients between SST and late monsoonal rainfall were 0.545 and −0.529 in the areas of positive and negative correlation, respectively. The SST dipole difference (positive – negative) was positively correlated with late monsoonal rainfall ($r = 0.604$). Use of the temperate southeastern Pacific SST dipole therefore increased the magnitude of the best single correlation coefficient by $0.604 - 0.545 = 0.059$. Rainfall during the early monsoon, inter-monsoon, and late monsoon were therefore teleconnected with no time lag to SSTs over the Pacific Ocean. In addition to the Pacific Ocean, SSTs in some areas of the Indian and Atlantic oceans were teleconnected with early and late monsoonal rainfall, respectively.

The real-time teleconnections between the monsoonal rainfall and SSTs in some areas of the Pacific Ocean are remarkable. Especially noteworthy are the negative correlations between early monsoonal rainfall and SSTs over the eastern equatorial Pacific and the eastern Pacific Ocean off Peru during La Niña conditions.

4.5. Teleconnections at lags of several months

We considered correlations with lag times of several months to be most desirable for predicting monsoonal rainfall. The left side of Fig. 8 shows significant correlations with SSTs at lags of 6, 8, and 9 months. There were significant positive correlations with early monsoonal rainfall southwest of Madagascar in the western Indian Ocean and off Argentina in the South Atlantic Ocean. There were significant negative correlations in the vicinity of the Antarctic Convergence south of South Africa. There were significant negative correlations between rainfall during the inter-monsoon and SST in the North Atlantic off Western Europe. There were significant positive correlations between rainfall during the

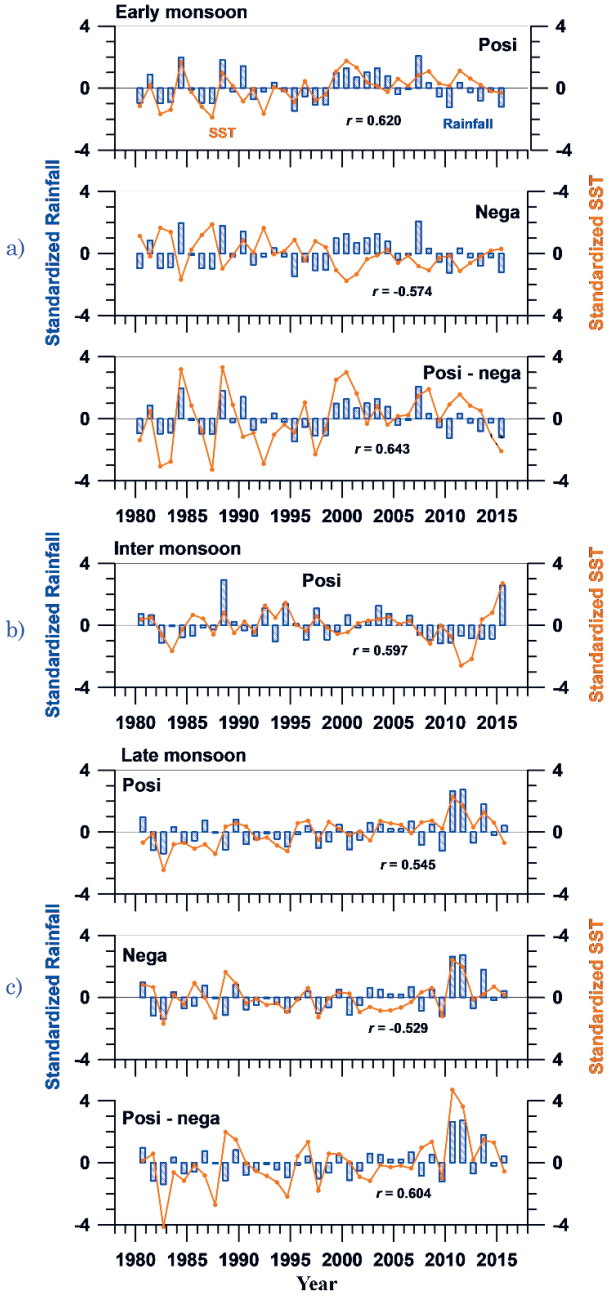

Figure 7. Standardized early monsoon rainfall and standardized SST in the focus areas for real-time correlations. (*a*) Early monsoon. (*b*) Inter-monsoon. (*c*) Late monsoon. In (*a*) and (*c*), a pair of areas where correlations were positive and negative was selected, and a third time series.

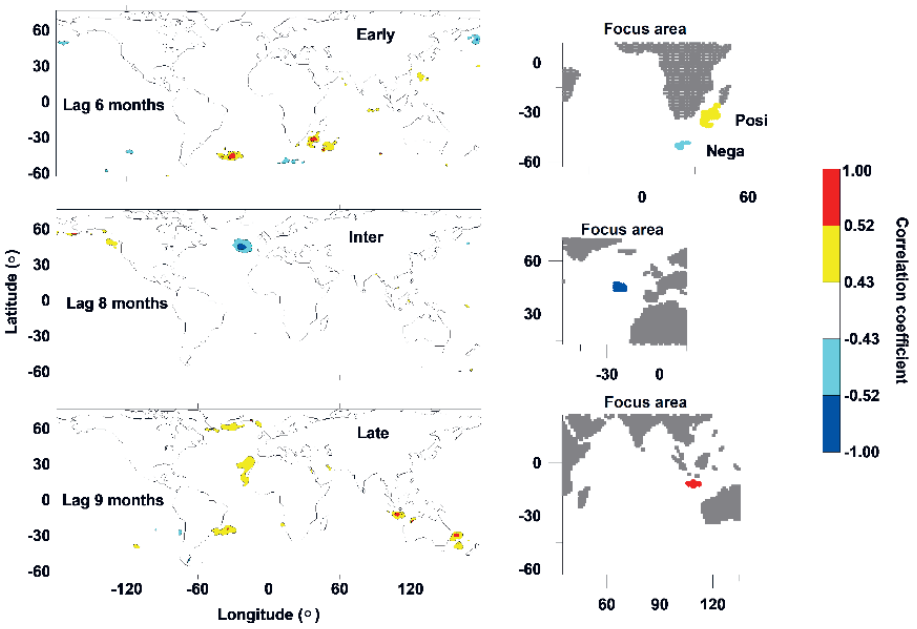

Figure 8. Similar to Fig. 6, but for time lags of 6 (early monsoon), 8 (inter-monsoon), and 9 (late monsoon) months.

late monsoon and SSTs in the East Indian Ocean south of Indonesia and in the South Pacific off the east coast of Australia.

The right side of Fig. 8 shows the central regions of some of the areas where the time-lagged correlations were significant, and Fig. 9 shows time series of the spatially averaged SSTs in the central regions (right side of Fig. 8) and monsoonal rainfall. For the early monsoon, the dipole difference (positive − negative) of the SSTs is shown in addition to the SSTs in the zones of positive and negative correlation. The correlation coefficients between the SSTs and early monsoonal rainfall in the areas of positive and negative correlation were 0.580 and −0.480, respectively. The correlation coefficient for the SST difference was 0.687 and exceeded the magnitude of the best positive or negative correlation coefficient by 0.107. The correlation coefficients between the SSTs in the core zones and the inter-monsoonal and late monsoonal rainfall were −0.561 and 0.592, respectively. Rainfall during the early monsoon was teleconnected with SST in the western Indian Ocean and rainfall during the late monsoon was teleconnected with SST in the eastern Indian Ocean after time lags of 6 and 9 months, respectively.

Myanmar faces the Indian Ocean, and water that evaporates from the Indian Ocean is the source of rainfall in the rainy season. The SST of the Indian Ocean is therefore expected to affect the rainfall during the rainy season (Sein et al. 2015; Toe et al. 2017). Rainfall during the early monsoon is negatively cor-

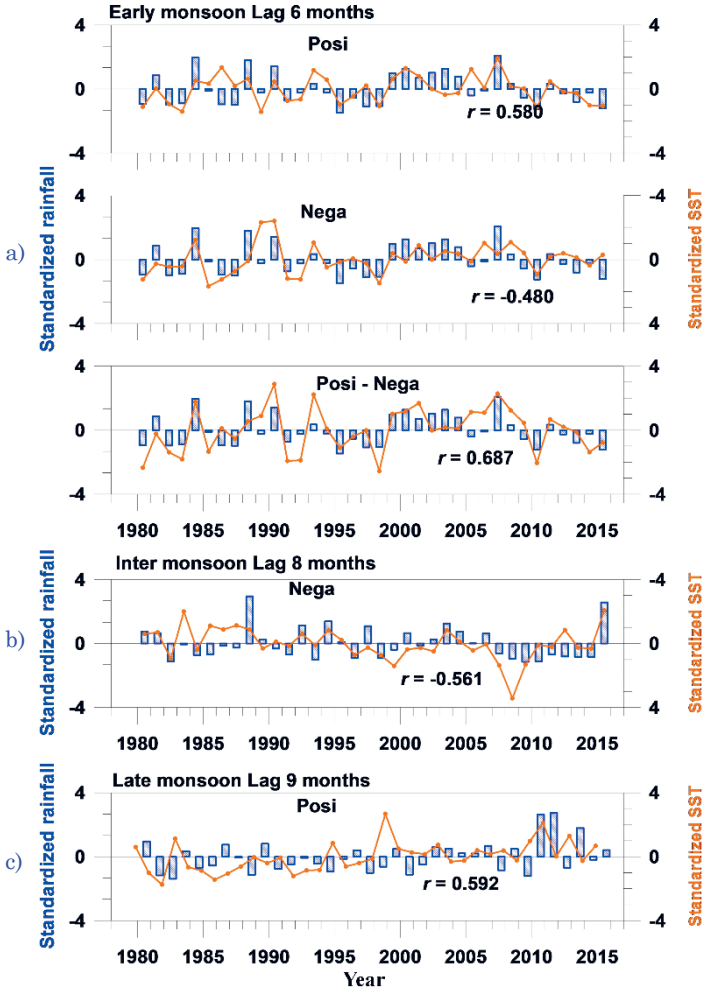

Figure 9. Similar to Fig. 7. (*a*) Early monsoon for a time lag of 6 months. The SST dipole is shown. (*b*) Inter-monsoon for a time lag of 8 months. (*c*) Late monsoon for a time lag of 9 months. (*a*). Inter-monsoon for time lag of 8 months (*b*). Late monsoon for time lag of 9 months (*c*).

related with the SST in the western Indian Ocean in real time and positively correlated with a lag of 6 months. Rainfall during the late monsoon is positively correlated with SST in the eastern Indian Ocean at a lag of 9 months.

4.6. Prediction of monsoonal rainfall from teleconnections with the ANN model

Teleconnections between rainfall in other countries and SST in certain parts of the ocean have been identified, and rainfall predictions have been performed with an ANN model (Yuan et al., 2016; Alhamshry et al., 2019). By using SSTs

several months prior to the monsoon, we predicted rainfall with the ANN model. To predict early monsoonal rainfall with the ANN, we used the SST time series at the bottom of Fig. 9a (SST difference) as the input of the ANN model (Fig. 2) and the early monsoonal rainfall as the output. To predict the inter-monsoonal and late monsoonal rainfall, we used the SST time series in Figs. 9b and 9c. As described in section 3.4., the model was optimized with the 1980–1997 time series and applied to the 1998–2015 time series.

Predicted monsoonal rainfall generally followed the trend of the observed rainfall. The correlation coefficients between the predicted and observed rainfall exceeded 0.7 (Fig. 10). The predicted early monsoonal rainfall correctly reproduced the wet period from 1999 to 2008 and the dry period from 2012 to 2015. The predicted inter-monsoonal rainfall reproduced the dry period from 2007 to 2014 and the abrupt increase of rainfall in 2015. The predicted late monsoonal

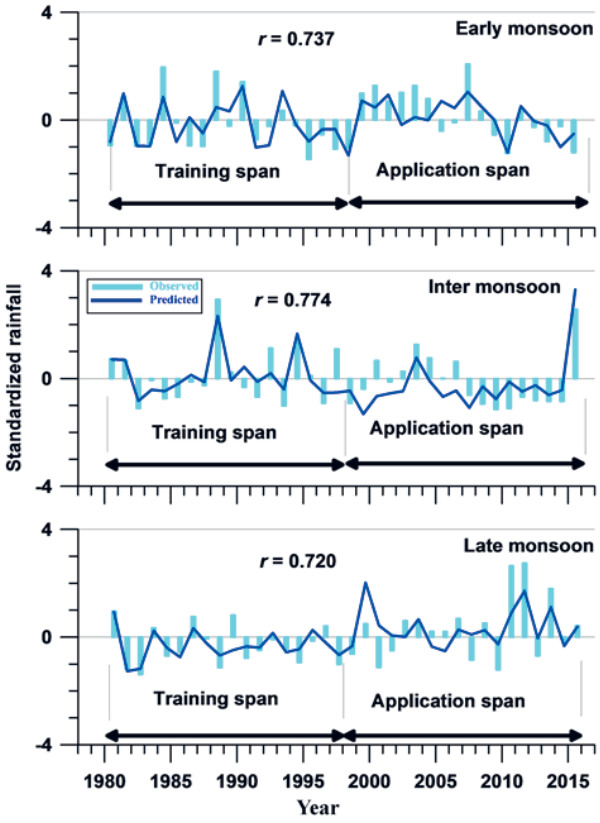

Figure 10. Comparison of standardized observed monsoonal rainfall with standardized rainfall predicted by the artificial neural network model.

rainfall reproduced the wet period from 2011 to 2014. The ANN model could therefore predict monsoonal rainfall in the CDZ based on SST zones in the ocean 6–9 months prior to the monsoon.

5. Conclusions

The goal of this study was to reveal the characteristics of rainfall over the CDZ of Myanmar. Because the rainy season is divided into two parts (the early and late monsoon) by the inter-monsoon, rainfed agriculture is difficult to sustain. To find a way to predict rainfall, the teleconnections between the SSTs in different parts of the ocean and monsoonal rainfall were examined. The monsoonal rainfall was successfully predicted with an ANN.

1. In the CDZ of Myanmar, average rainfall during July (34.9 mm) is inadequate for rainfed agriculture, and the rainfall is highly variable. Rainfed agriculture is therefore difficult to sustain in the CDZ.

2. The monthly mean rainfall follows a bimodal pattern. We divided the summer monsoon, which lasts from May to October, into an early monsoon (May–June) and late monsoon (August–October) separated by an inter-monsoon (July). There is very little correlation between the early and late monsoonal rainfall ($r = -0.257$).

3. There are teleconnections between the rainfall during the early monsoon, inter-monsoon, and late monsoon and SSTs in areas of the Pacific Ocean in real time. At lag times of several months, there are teleconnections between the early monsoonal, inter-monsoonal, and late monsoonal rainfall and SSTs in areas of the Indian and Atlantic Ocean. In real time, there were teleconnections between monsoonal rainfall and SSTs in the Pacific Ocean (Fig. 6), and at time lags of 6–9 months, there were teleconnections between monsoonal rainfall and SSTs in the Indian and Atlantic Ocean (Fig. 8).

4. Using the teleconnections with SST at time lags of 6–9 months, we were able to predict monsoonal rainfall with an Elman-type ANN model. Correlation coefficients between the observed and predicted rainfall exceeded 0.7.

Acknowledgements – The authors gratefully acknowledge the financial support of the Joint Research Program of the Arid Land Research Centre, Tottori University (No. 29A2001). The authors gratefully acknowledge the help of Mr. Tatsuo Fujimura (MJET, Tokyo) in obtaining data and information.

Conflict of interest statement – The authors have no conflicts of interest in relation to this study.

References

Ahmed, A. O. C., Yasuda, H., Hattori, K. and Nagasawa, R. (2008): Analysis of rainfall records (1923–2004) in Atar-Mauritania, *Geofizika,* **25**, 53–64.

Alhamshry, A. A. T., Fenta, A. A., Yasuda, H., Shimizu, K. and Kawai, T. (2019): Prediction of summer rainfall over the source region of the Blue Nile by using teleconnections based on sea surface temperatures, *Theor Appl. Climatol.*, https://doi.org/10.1007/s00704-019-02796-x.

Alhamshry, A., Fenta, A. A., Yasuda, H., Kimura, R. and Shimizu, K. (2020): Seasonal rainfall variability in Ethiopia and its long-term link to global sea surface temperatures, *Water,* **12**, 55, https://doi.org/10.3390/w12010055.

Asian Development Bank (2016): Climate risk and vulnerability assessment, in: *Project Number 47152*, May 2016, Nay Pyi Taw, 24 pp.

Bishop, C. M. (1995): *Neural networks for pattern recognition*. Oxford University Press, New York.

Bonaccorso, B., Cancelliere, A. and Rossi, G. (2003): An analytical formulation of return period of drought severity, *Stoch. Environ. Res. Risk. Assess.*, **17**, 157–174, http://doi.org/10.1007/s00477-003-0127-7.

Chhin, R., Shwe, M. M. and Yoden, S. (2019): Time-lagged correlations associated with interannual variations of pre-monsoon and post-monsoon precipitation in Myanmar and the Indochina Peninsula, *Int. J. Climatol.,* **40**, 3792–3812, https://doi.org/10.1002/joc.6428.

Dash, N. B., Panda, S. N., Remesan, R. and Sahoo, N. (2010): Hybrid neural modeling for groundwater level prediction, *Neural Compt. Appl.,* **19**, 1251–1263, https://doi.org/10.1007/s00521-010-0360-1.

Deka, R. L. and Nath, K. K. (2000): Rainfall analysis for rainfed crop planning in the Upper Brahmaputra Valley Zone of Assam, *J. Agrometeorol.,* **2**, 47–53.

Eagleson, P. S. (1970): *Dynamic hydrology*. McGraw-Hill Book Company New York.

Elman, J. L. (1990): Finding structure in time, *Cogn. Sci.*, **14**, 179–121, https://doi.org/10.1207/s15516709cog1402_1.

Food and Agriculture Organization of the United Nations and Earthscan (2011): *The state of the world's land and water resources for food and agriculture*. Earthscan, Abingdon.

Goyal, M. K. and Ojha, C. S. P. (2012): Downscaling of surface temperature for lake catchment in an arid region in India using linear multiple regression and neural networks, *Int. J. Climatol.,* **32**, 552–566, https://doi.org/10.1002/joc.2286.

Graef, F. and Haigis, J. (2001): Spatial and temporal rainfall variability in the Sahel and its effects on farmers' management strategies, *J. Arid. Environ.,* **48**, 221–231, https://doi.org/10.1006/jare.2000.0747.

Herridge, D. F., Win, M. M., New, K. M., Kyu, K. L., Win, S. S., Shwe, T., Min, Y. Y., Denton, M. D. and Cornish, P. S. (2019): The cropping systems of the Central Dry Zone of Myanmar: Productivity constraints and possible solutions, *Agri. Syst.*, **169**, 31–40, https://doi.org/10.1016/j.agsy.2018.12.001.

Japan International Cooperation Agency (2010): *The development study on sustainable agriculture and rural development for poverty reduction programme in the central dry zone of the union of Myanmar*, Final Report.

Kumbuyo, C., Yasuda, H., Kitamura, Y. and Shimizu, K. (2014): Fluctuation of rainfall time series in Malawi: An analysis of selected areas, *Geofizika*, **31**, 13–34, https://doi.org/10.15233/gfz.2014.31.1.

Lloyd-Hughes, B. and Saunders, M. A. (2002): Seasonal prediction of European spring precipitation from El Nino Southern Oscillation and local sea-surface temperatures, *Int. J. Climatol.*, **22**, 1–14, https://doi.org/10.1002/joc.723.

Mondal, P, Srivastav, P, Kalin, L. and Panda, S. N. (2011): Ecologically sustainable surface water withdrawal for cropland irrigation through incorporation of climate variability, *J. Soil Water Conserv.*, **66,** 221–232, https://doi:10.2489/jswc.66.4.221.

Nyakudya, I. W. and Stroosnijder, L. (2011): Water management options based on rainfall analysis for rainfed maize (Zea mays L.) production in Rushinga district, Zimbabwe, *Agr. Water Manage.*, **98**, 1649–1659, https://doi.org/10.1016/j.agwat.2011.06.002.

Olsson, J., Uvo, C. B. and Jinno, K. (2001): Statistical atmospheric downscaling of short-term extreme rainfall by neural networks, *Phys. Chem. Earth Pt. B.*, **26**, 695–700, https://doi.org/10.1016/S1464-1909(01)00071-5.

Poe, C. A. (2011): *Food Security Assessment in the Dry Zone Myanmar*. WFP, Food Security Analysis Services, 29 pp.

Rayner, N. A., Parker, D. E., Horton, E. B., Folland, C. K., Alexander, L. V., Rowell, D. P., Kent, E. C. and Kaplan, A. (2003): Global analyses of sea surface temperature, sea ice, and night marine air temperature since the late nineteenth century, *J. Geophys. Res.*, **108**, D14, https://doi.org/10.1029/2002JD002670.

Rayner, N. A., Brohan, P., Parker, D. E., Folland, C. K., Kennedy, J. J., Vanicek, M., Ansell, T. and Tett, S. F. B. (2006): Improved analyses of changes and uncertainties in sea surface temperature measured in situ since the mid-nineteenth century: The HadSST2 data set, *J. Clim.*, **19**, 446–469, https://doi/10.1175/JCLI3637.1.

Roy, N. S. and Kaur, S. (2000): Climatology of monsoon rains of Myanmar (Burma), *Int. J. Climatol.*, **20**, 913–928, https://doi.org/10.1002/1097-0088(20000630)20:8<913::AID-JOC485>3.0.CO;2-U.

Roy, S. S. and Roy, N. S. (2011): Influence of Pacific decadal oscillation and El Niño Southern oscillation on the summer monsoon precipitation in Myanmar, *Int. J. Climatol.*, **31**, 14–21, https://doi:10.1002/joc.2065.

Rugumayo, A. I. and Mwebaze, D. B. (2007): Drought-intensity duration and frequency analysis: A case study of Western Uganda, *Water Environ. J.*, **16**, 11–15, https://doi.org/10.1111/j.1747-6593.2002.tb00380.x.

Sein, Z. M. M., Ogwang, B. A., Ongoma, V., Ogou, F. K. and Batebana, K. (2015): Inter-annual variability of summer monsoon rainfall over Myanmar in relation to IOD and ENSO, *J. Env. Agri. Sci.*, **4**, 28–36.

Sfersos, A. and Coonick, A. H. (2000): Univariate and multivariate forecasting of hourly solar radiation with artificial intelligence techniques, *Sol. Energy,* **68**, 169–178, https://doi.org/10.1016/S0038-092X(99)00064-X.

Shahi, N. K., Rai, S. and Sahai, A. K. (2020): The relationship between the daily dominant monsoon modes of South Asia and SST, *Theor. Appl. Climatol.*, **142**, 59–70, https://doi.org/10.1007/s00703-021-00793-2.

Shahi, N. K., Rai, S. and Mishra, N. (2019): Recent predictors of Indian summer monsoon based on Indian and Pacific Ocean SST, *Meteorol. Atmos. Phys.*, **131**, 525–539, https://doi.org/10.1007/s00703-018-0585-6.

Shahi, N. K., Rai, S., Sahai, A. K. and Abhilash, S. (2018): Intra-seasonal variability of the South Asian monsoon and its relationship with the Indo–Pacific sea-surface temperature in the NCEP CFSv2, *Int. J. Climatol.*, **38**, e28–e47, https://doi.org/10.1002/joc.5349.

Shahi, N. K., Rai, S. and Pandey, D. K. (2016): Prediction of daily modes of South Asian monsoon variability and its association with Indian and Pacific Ocean SST in the NCEP CFS V2, *Meteorol. Atmos. Phys.*, **128**, 131–142, https://doi.org/10.1007/s00703-015-0404-2.

Singh, K. A., Sikka, A. K. and Rai, S. K. (2008): Rainfall distribution pattern and crop planning at Pusa in Bihar, *J. Agrometeorol.*, **10**, 198–203.

Smith, I. N., McIntosh, P., Ansell, T. J., Reason, C. J. C. and McInnes, K. (2000): Southwest western Australian winter rainfall and its association with ocean climate variability, *Int. J. Climatol.*, **20**, 1913–1930, https://doi.org/10.1002/1097-0088(200012)20:15<1913::AID-JOC594>3.0.CO;2-J.

Takahashi, H. G. and Yasunari, T. (2006): A climatological monsoon break in rainfall over Indochina – A singularity in the seasonal march of the Asian summer monsoon. *J. Climate,* **19**, 1545–1556, https://doi:10.1175/JCLI3724.1.

Toe, M. T., Kanzaki, M., Lien, T. H. and Cheng, K. S. (2017): Spatial and temporal rainfall patterns in Central Dry Zone, Myanmar – A hydrological cross-scale analysis, *Terr. Atmos. Ocean Sci.*, **28**, 425–436, https://doi.org/10.3319/TAO.2016.02.15.01(Hy).

Uvo, C. B., Repelli, C. A., Zebiak, S. E. and Kushnir, Y. (1998): The relationships between tropical Pacific and Atlantic SST and northeast Brazil monthly precipitation, *J. Clim.*, **11**, 51–562, https://doi.org/10.1175/1520-0442(1998)011<0551:TRBTPA>2.0.CO;2.

Uvo, C. B., Tölle, U. and Berndtsson, R. (2000): Forecasting discharge in Amazonia using artificial neural networks, *Int. J. Climatol.*, **20**, 1495–1507, https://doi.org/10.1002/1097-0088(200010)20:12<1495::AID-JOC549>3.0.CO;2-F.

Yasuda, H., Panda, S. N., Abd Elbasit, M. A. M., Kawai, T., El Gamri, T., Fenta, A. A. and Nawata, H. (2018): Teleconnection of rainfall time series in the central Nile Basin with sea surface temperature, *Paddy Water Environ.*, **16**, 805–821, https://doi.org/10.1007/s10333-018-0671-x.

Yasunari, T (1990): Impact of Indian monsoon on the coupled atmosphere/ocean system in the tropical Pacific, *Meteorol. Atmos. Phys.,* **44**, 29–41.

Yuan, F., Berndtsson, R, Uvo, C. B., Zhang, L. and Jiang, P. (2016): Summer precipitation prediction in the source region of the Yellow River using climate indices, *Hydrol. Res.*, **47**, 847–856, https://doi.org/10.2166/nh.2015.062.

Yusof, F., Hui-Mean, F., Suhaila, J. and Yusof, Z. (2013): Characterisation of drought properties with bivariate copula analysis, *Water Resour. Manag.*, **27**, 4183–4207, https://doi.org/10.1007/s11269-013-0402-4.

SAŽETAK

Predviđanje bimodalne monsunske oborine u središnjem dijelu sušne zone Mianmara na temelju daljinske povezanosti s globalnim površinskim temperaturama mora

Hiroshi Yasuda, Ayele Almaw Fenta, Hidetoshi Miyazaki, Shun Ishiyama, Koji Inosako, Aung Din i Takayuki Kawai

U središnjem dijelu sušne zone Mianmara prosječna je godišnja količina oborine manja od 1000 mm. Poljoprivreda se ondje uobičajeno oslanja na dostupnost oborinske vode te je ona stoga značajno ugrožena njenim velikim oscilacijama i čestim pojavama sušnih godina. Mjesečna raspodjela oborine ima bimodalni karakter. Obilježje intenziteta monsunske oborine od svibnja do listopada je pojava dvaju maksimuma: rani (svibanj–lipanj) i kasni (kolovoz–listopad) koji su razdvojeni među-monsunom (srpanj). Upravljanje poljoprivredom koja se oslanja na oborinu je problematično zbog povratnih perioda sušnih i vlažnih godina. Postoji vrlo slaba korelacija između rane i kasne monsunske oborine ($r = -0{,}257$). Međutim, uočava se daljinska povezanost monsunske oborine s površinskim temperaturama mora (SST) određenih područja Tihog oceana. Nadalje, postoji i povezanost između rane monsunske, među-monsunske i kasne monsunske oborine i SST-a određenih područja Indijskog oceana i Atlantskog oceana s odmakom od 6 do 9 mjeseci. Koristili smo Elmanov model umjetne neuronske mreže za predviđanje rane monsunske, među-monsunske i kasne monsunske oborine na temelju daljinske povezanosti sa SST-em Indijskog i Atlantskog oceanu s pomakom od 6 do 9 mjeseci. Koeficijent korelacije između predviđene i opažene količine oborine premašio je 0,7 u sva tri slučaja.

Ključne riječi: umjetna neuronska mreža, bimodalna oborina, među-monsun, središnje područje sušne zona Mianmara, poljoprivreda ovisna o oborini

Corresponding author's address: Hiroshi Yasuda, Organization for Educational Support and International Affairs, Tottori University, Koyama Minami 4-101, Tottori 680-8550, Japan; e-mail: hiroshiyasudag@gmail.com